OPEN

New Prospects for Ultra-High-Field Magnetic Resonance Imaging in Multiple Sclerosis

Benjamin V. Ineichen, MD, PhD,† Erin S. Beck, MD, PhD,**
*Marco Piccirelli, PhD,† and Daniel S. Reich, MD, PhD**

Abstract: There is growing interest in imaging multiple sclerosis (MS) through the ultra-high-field (UHF) lens, which currently means a static magnetic field strength of 7 T or higher. Because of higher signal-to-noise ratio and enhanced susceptibility effects, UHF magnetic resonance imaging improves conspicuity of MS pathological hallmarks, among them cortical demyelination and the central vein sign. This could, in turn, improve confidence in MS diagnosis and might also facilitate therapeutic monitoring of MS patients. Furthermore, UHF imaging offers unique insight into iron-related pathology, leptomeningeal inflammation, and spinal cord pathologies in neuroinflammation. Yet, limitations such as the longer scanning times to achieve improved resolution and incipient safety data on implanted medical devices need to be considered. In this review, we discuss applications of UHF imaging in MS, its advantages and limitations, and practical aspects of UHF in the clinical setting.

Key Words: ultra-high-field, 7 T, magnetic resonance imaging, multiple sclerosis, neuroimaging, review, paramagnetic rim, central vein sign, cortical lesions, leptomeningeal enhancement

(*Invest Radiol* 2021;56: 773–784)

MULTIPLE SCLEROSIS

Clinical Phenotypes of Multiple Sclerosis

Multiple sclerosis (MS) is the most common neuroinflammatory disease.[1] In most cases, it is defined by bouts of partially or fully reversible neurological disability. In many patients, after a disease course of 10 to 20 years, this relapsing-remitting disease stage converts to a secondary progressive disease stage. A minority of MS patients presents with a primary progressive disease course.

Received for publication March 26, 2021; and accepted for publication, after revision, May 9, 2021.

From the *Translational Neuroradiology Section, National Institute of Neurological Disorders and Stroke, National Institutes of Health, Bethesda, MD; and †Department of Neuroradiology, Clinical Neuroscience Center, University Hospital Zurich, University of Zurich, Zurich, Switzerland.

Conflicts of interest and sources of funding: none declared.

This work was supported by a grant from the University of Zurich (FK-20-050) and by the Intramural Research Program of National Institute of Neurological Disorders and Stroke, National Institutes of Health. No funding was received specifically for the publication of this article.

Correspondence to: Benjamin V. Ineichen, MD, PhD, Translational Neuroradiology Section, National Institute of Neurological Disorders and Stroke, National Institutes of Health, Room 5C101A, Bldg 10, 10 Center Dr, Bethesda, MD 20892-4128. E-mail: ineichen@protonmail.ch; Daniel S. Reich, MD, PhD, Translational Neuroradiology Section, National Institute of Neurological Disorders and Stroke, National Institutes of Health, Room 5C103, Bldg 10, 10 Center Dr, Bethesda, MD 20892-4128. E-mail: daniel.reich@nih.gov.

ISSN: 0020-9996/21/5611–0773
DOI: 10.1097/RLI.0000000000000804

Pathological Hallmarks of Multiple Sclerosis

Multiple sclerosis pathology affects different intracranial compartments, with white matter pathology being most readily recognizable on magnetic resonance imaging (MRI) (Fig. 1). This white matter pathology is defined by the emergence of multiple inflammatory and demyelinating lesions with concomitant axonal degeneration[2,3] (Fig. 1A). The formation of these lesions is preceded by local breakdown of the blood-brain barrier with subsequent infiltration of immune cells, which emigrate from venules and spread in a centrifugal manner around the vessel (Fig. 1B). Such white matter lesions can be grouped according to inflammatory activity,[4] and a minority of these lesions can also show extensive remyelination.[5–7]

In addition to white matter pathology, MS also shows pronounced pathology within the gray matter, which was initially described in the 19th century.[8] Yet recognition of the relevance of gray matter pathology in MS has only recently gained momentum[9–17]: several studies have demonstrated that cortical pathology is closely linked to clinical disability[18,19] (reviewed in Calabrese et al[20]). Based on this work, in 1 scheme based on histopathology, cortical MS lesions were classified into 4 subtypes[21]: (1) leukocortical lesions, appearing at the interface between white and gray matter; (2) intracortical lesions, emerging radially from cortical venules; (3) subpial lesions, in which demyelination along the gyral surface extends no deeper than cortical layers 3 or 4, and which are hypothesized to be a specific feature of MS[22]; and (4) cortex-spanning lesions, affecting the entire cortical band (Fig. 1C). The origin of cortical pathology is still a matter of debate.[20] Leptomeningeal inflammation has been suggested as a driver of overall cortical MS pathology[11,23] and/or subpial MS lesions (class III)[24] due to the spatial association between cortical MS pathology and leptomeningeal inflammation in postmortem histopathology studies. Meningeal inflammatory aggregates contain immune cells, including T cells, B cells, plasma cells, and macrophages[25] (Fig. 1D). In addition, the meninges are a site of ectopic tertiary lymphoid tissue genesis, organized into B-cell follicle-like structures.[23,24,26] The exact mechanism linking meningeal inflammation and cortical pathology remains unclear, but it has been suggested that inflammatory cytokines in the cerebrospinal fluid (CSF), excreted by these follicles, induce subpial demyelination[24,26–28] (reviewed in Zurawski et al[9]).

Together, these pathological features contribute to diffuse neurodegeneration in MS, particularly pronounced during the progressive disease stage.[29] Other factors have also been linked to neurodegeneration in MS, among them brain tissue iron accumulation[30–32] (Fig. 1E), microglial activation,[10] mitochondrial dysfunction,[33] and oxidative burst[34] (reviewed in Mahad et al[29]). This incremental neurodegeneration and diffuse tissue injury ultimately results in accumulating brain and spinal cord tissue loss.[35] Importantly, both brain and spinal cord atrophy are closely linked to clinical disability.[36,37]

MAGNETIC RESONANCE IMAGING IN MULTIPLE SCLEROSIS IN THE CLINICAL SETTING

The Role of Magnetic Resonance Imaging in Multiple Sclerosis Diagnosis and Therapeutic Monitoring

As evident from pathology studies, MS is a central nervous system (CNS)–wide disease with a chronic course. These hallmarks are

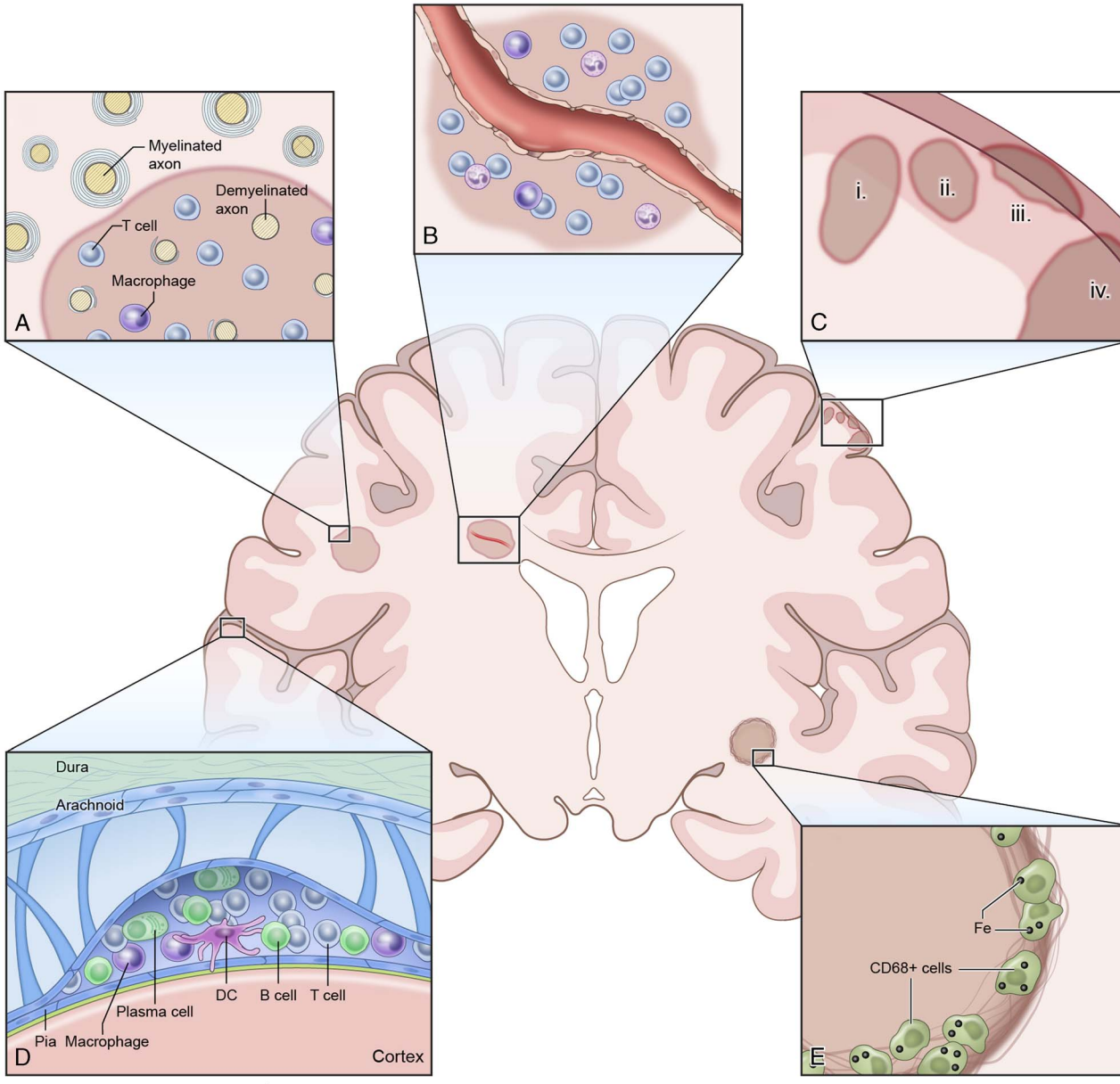

FIGURE 1. Pathologic hallmarks of multiple sclerosis (MS). Multiple sclerosis is defined by focal inflammatory and demyelinating white matter lesions (A), frequently forming around a centrally located vein (B). Multiple sclerosis pathology also affects gray matter including the cortical ribbon; cortical lesions have been phenotypically classified into (1) leukocortical lesions, (2) intracortical lesions, (3) subpial lesions, and (4) cortex-spanning lesions (C). Multiple sclerosis pathology also affects the leptomeningeal compartment, as defined by cellular infiltrates and/or lymphoid follicles (D). The inflammatory front of chronic active white matter lesions can show iron-laden phagocytes (E).

reflected in the diagnostic criteria of MS. The McDonald criteria were originally introduced in 2001[38] and underwent several revisions, most recently in 2017.[39] These criteria identify MS or a high likelihood of the disease in patients with typical clinically isolated syndrome (CIS),[40] that is, monophasic clinical episodes with patient-reported symptoms and objective findings reflecting an inflammatory demyelinating event in the CNS.[41] Diagnosis requires the fulfillment of 2 criteria: (1) dissemination in time: at least 2 distinct episodes suggestive of MS in the patient history; and (2) dissemination in space: neuroinflammatory damage in different CNS regions.

Because there is no single pathognomonic clinical feature or diagnostic test for MS, the McDonald criteria integrate clinical, imaging, and laboratory findings. However, MRI has gained particular momentum in the MS diagnosis[42] and to rule out common MS mimics.[43] With this, brain and spinal cord MRI remain the most important paraclinical tests to substantiate MS diagnosis,[39] not least due to its ability to sensitively visualize white matter pathology.

Magnetic resonance imaging can be used to determine both dissemination in time and space. Dissemination in time can be confirmed by the simultaneous presence of non–gadolinium-enhancing and gadolinium-enhancing lesions in the CNS or by a new T2-weighted (T2w) hyperintense or T1w contrast-enhancing lesion on a follow-up MRI scan. Dissemination in space can be confirmed by 1 or more T2w hyperintense lesions in 2 or more of 4 characteristic CNS sites, that

is, (juxta)cortical, periventricular, infratentorial, and/or spinal cord. Magnetic resonance imaging can also support the identification of mechanisms behind disease progression, including paramagnetic rim lesions, subpial demyelination, distinct spinal cord pathology, and brain and spinal cord atrophy.[44]

Besides its critical role in MS diagnosis, MRI also has a key role in therapeutic monitoring of MS upon initiation of disease-modifying therapy.[45] The most commonly used treatment response measure is new or enlarging lesions on T2w MRI scans.[46] Gadolinium-enhancing lesions are another frequently used surrogate marker for clinical activity, but accumulation of new T2w lesions more sensitively gauges subclinical disease activity,[47] especially when assessed using image subtraction. Finally, it is undisputed that brain and spinal cord atrophy can aid in monitoring disease activity,[45,48] yet quantifying atrophy in the clinical setting is still at risk of substantial confounding factors caused by physiological (eg, diurnal brain size fluctuation, hydration state) or technical parameters (eg, acquisition protocols, gradient distortion, or intrascanner/interscanner variability) (reviewed in Sastre-Garriga et al[48]).

Limitations of Multiple Sclerosis Magnetic Resonance Imaging at Clinical Field Strengths

Early MS treatment is associated with better long-term outcomes,[49] making early diagnosis key for effective patient management. Yet the pressure to diagnose MS early frequently results in misdiagnosis, which can have serious health and financial consequences.[50] Given this, it is noteworthy that the McDonald criteria do not address differentiating MS from other disorders.[39] Instead, the focus of the 2017 revision of the McDonald criteria optimizes sensitivity over specificity. In fact, several studies have found suboptimal specificity of the current McDonald criteria for MS diagnosis; these include a retrospective Chinese study including 93 CIS patients, which detected 75% sensitivity but only 47% specificity upon usage of the 2017 McDonald criteria,[51] and a prospective Indian study comprising 82 CIS patients, which showed a specificity of 79%.[52]

The limited specificity of the current McDonald criteria is partially due to the nonspecific nature of white matter lesions, the imaging hallmark of MS diagnosis. Whereas white matter lesions due to MS often share features such as abutting the lateral ventricles or an ovoid shape,[53] they can be difficult to distinguish from white matter lesions with a different underlying pathology. As a consequence, several neurological disorders can imitate inflammatory demyelination, most commonly other diseases with white matter lesions, such as migraine, fibromyalgia, neuromyelitis optica spectrum disorder,[54] and chronic microvascular ischemic disease.[40] With this, the MS misdiagnosis rate has been reported to be on the order of 20%.[55] Thus, having more specific features for MS diagnosis would be paramount to increase specificity of MS diagnosis.

Several imaging biomarkers with good specificity for MS have been proposed in recent years, among them the central vein sign (CVS).[56] This MRI-detectable vein inside white matter lesions seems to represent the centrally located vein within an MS lesion from which immune cells spread radially to the parenchyma.[57] The CVS is readily detectable on T2*w scans due to the paramagnetic properties of venous blood.[58] It is increasingly acknowledged as being supportive for an MS diagnosis.[59–61] Also, cortical lesions, particularly subpial lesions, may be a specific MS feature,[53] and they can also be an imaging feature of progressive MS.[44] Yet, imaging at clinical field strength, that is, 1.5 or 3 T, has very poor sensitivity to cortical lesions. A recent postmortem MRI histopathology study showed that clinical MRI scratches the surface of cortical lesions: a maximum of 24% of cortical lesions may be detected using phase-sensitive inversion recovery (PSIR) or double inversion recovery (DIR) sequences at 3 T.[62] The sensitivity for cortical lesion detection is expected to be even lower in the clinical setting. Increasing sensitivity of cortical lesion display would not only aid MS diagnosis but would also support treatment monitoring due to the close association between cortical lesions and clinical disability. This is also supported by the fact that cortical MS lesions are associated with cognitive impairment independent of white matter lesions.[63,64]

Other important CNS sites include the optic nerve and spinal cord. The optic nerve has been proposed as a fifth anatomical location to fulfill the dissemination in space dimension from the McDonald criteria,[42] and increased sensitivity to detect lesions in this small anatomical compartment could further increase accuracy of MS diagnosis.[39] Finally, sensitivity of clinical spinal cord imaging to detect pathological changes is still insufficient despite spinal MS pathology being closely associated with clinical disability, particularly during the progressive MS disease stage.[65]

MAGNETIC RESONANCE IMAGING AT 7 T

Advantages of 7-T Magnetic Resonance Imaging for Multiple Sclerosis

Magnetic resonance imaging at a static magnetic field strength of 3 T was clinically introduced in the early 2000s.[66] These scanners are equipped with a platform of multichannel receive coils dedicated for various clinical questions. With this, they are still considered as the criterion standard in clinical MRI. Hence, imaging at 7 T—also termed ultra-high-field (UHF) MRI—competes with advanced clinical 3-T MRI and must thus offer a clear benefit translating into improved diagnostics or therapeutic monitoring.

For MS, UHF imaging offers 2 main advantages[1]: increased signal-to-noise ratio (SNR) and[2] enhanced susceptibility effects.[67] The SNR, that is, the ratio of the signal to background noise, increases proportionally with the static magnetic field strength. A recent brain imaging study even suggested that SNR might scale supralinearly with static magnetic field strength under certain conditions.[68] Further, the use of phased array coils at 7 T allows for parallel imaging[69,70] with reduced SNR penalty due to less intense far-field behavior.[71] This allows the use of higher parallel imaging acceleration factors than at lower fields. Sufficient imaging acceleration is key in the clinical setting due to time constraints and to keep motion artifacts to a minimum. The increase in SNR translates to enhanced tissue resolution and contrast-to-noise ratio, for example, for gray and white matter, which, in turn, enables more sensitive detection of CNS pathology such as cortical lesions. Of note also is that the shift between the water and fat signal also increases with the static magnetic field strength, potentially resulting in more chemical shift artifacts.[72,73]

Second, increased magnetic field strength emphasizes tissue susceptibility effects, that is, the induction of local variations of the magnetic field by tissues with slightly different magnetic properties.[74] These field distortions are particularly prominent near bones and air, but also in the vicinity of veins, which have high levels of deoxyhemoglobin,[75] and tissue with high iron levels.[76] This concept is harnessed in susceptibility-weighted imaging to sensitively image central veins in MS plaques,[77] paramagnetic rims of MS plaques,[78] and iron deposits.[79]

Value of 7-T Magnetic Resonance Imaging for Displaying Pathologic Features of Multiple Sclerosis

Gray Matter Pathology

Cortical MS lesions are notoriously difficult to visualize, likely due to their small dimension, lower baseline myelination of the cortex, low-inflammatory phenotype, and partial volume effects with CSF.[80] At 3 T, a recent postmortem study showed that fewer than a quarter of histopathologically confirmed cortical lesions could be depicted in T2w fluid-attenuated inversion recovery (T2-FLAIR), DIR, or PSIR sequences,[62] and these rates are likely much lower in the clinical setting. Observations from postmortem studies suggest that UHF imaging enhances sensitivity for cortical lesion detection up to approximately 30% to 40%, depending on the lesion type[14,81] (Table 1). Several

studies have directly compared sensitivity of cortical lesion detection at 3 versus 7 T in vivo. One study comprising 26 patients with CIS or MS and comparing 3-T DIR with 7-T FLASH T2*w found more cortical lesions using 7-T imaging.[82] These results were confirmed in a recent study including 20 MS patients.[83] A postmortem study in brain sections of 19 MS patients using T1w, T2w, T2-FLAIR, DIR, or T2*w further substantiated this finding.[14] Of note, this study found a similarly low sensitivity of 7% to detect subpial lesions for DIR both at 3 and 7 T. Results from 1 study suggested that 7-T T2-FLAIR shows higher sensitivity at detecting cortical lesions compared with DIR, T2w, or T1w images.[84]

Ultra-high-field imaging not only seems to improve sensitivity for cortical lesion detection but also facilitates classification of cortical lesions (Fig. 2). A study deploying both 3- and 7-T imaging in 11 MS/CIS patients found that 7 T was superior at confidently classifying the location of cortical lesions to cortical or subcortical boundaries.[85] Further, results from this study indicated that some of the DIR hyperintensities at 3 T, identified as cortical lesions, were actually areas of signal arising from extracortical blood vessels. A pioneering study in 16 MS patients showed that 7-T imaging allowed characterization of cortical plaques into types 1 to 4.[17] In a study with 26 MS patients, 7-T FLASH T2*w was more accurate at detecting particularly subpial lesions compared with 3-T DIR and magnetization-prepared rapid acquisition with gradient echo (MPRAGE).[82] Inversion recovery susceptibility-weighted imaging with enhanced T2 weighting is a T2*w sequence with suppressed CSF signal, which allows for improved detection of subpial lesions at 3 T,[86] but it has not yet been investigated at 7 T. Of note, a study comparing MP2RAGE and T2*w images at 7 T can show higher sensitivity of MP2RAGE to detect cortical lesions, albeit some lesions were only seen on T2*w images.[87] Because subpial lesions have been proposed as a pathognomonic feature of MS, classification of cortical lesions is particularly important to improve specificity of MRI for MS diagnosis.[88] The interrater agreement for cortical lesions is also improved in 7-T imaging compared with clinical field strengths.[82,85] Of note, a recently developed method for automated detection of cortical lesions at 7 T based on MP2RAGE as single image contrast could also benefit the clinical and research settings by avoiding tedious manual lesion segmentation.[89]

Importantly, cortical pathology seems to go beyond mere focal tissue damage caused by cortical lesions.[20] Several studies have alluded to more diffuse cortical tissue damage, similar to the concept of normal-appearing white matter. An UHF MRI surface-based analysis of T2* relaxation times in MS showed significant increases in MS, possibly representing local myelin and iron loss.[90] Intriguingly, these changes were mainly confined up to 25% depth of the cortex. Although such measurements are at risk of partial volume effects with CSF, this finding supports the hypothesis that cortical pathology is driven from the pial surface, for example, via inflammatory cytokines within the CSF. Several other studies have also supported this notion.[24,64,91]

Multiple sclerosis also affects subcortical gray matter structures, such as the thalamus. However, the relative sensitivity of 7-T imaging for subcortical gray matter pathology has not been investigated extensively to date, despite its high clinical relevance.[92] One study including 12 MS patients showed improved detection of deep gray matter pathology in MS using T2*w imaging at 7 T.[93]

TABLE 1. Synopsis of the Role of UHF MRI (ie, MRI at 7-T Static Magnetic Field Strength) to Detect Pathologic Hallmarks of MS

MS Pathology	Role of UHF (7 T) MRI
Gray matter pathology	Increased detection of cortical MS lesions compared with 3 T Improved classification of cortical lesions compared with 3 T Potentially higher sensitivity to detect subcortical gray matter MS pathology (scarce evidence)
White matter pathology	Currently, at worst similar sensitivity to detect white matter lesions
CVS	Offers superior conspicuity of veins, enhancing evaluation of the CVS in more difficult MS cases, eg, with only small lesions
LME	Insights into LME pathology, eg, patterns of LME ("nodular" versus "spread/fill") Unclear if higher sensitivity to detect LME compared with 3 T (no comparative studies)
Focal/diffuse iron deposition	Insights into iron pathophysiology, eg, iron tissue content
Spinal cord pathology	Improved sensitivity to detect spinal cord MS lesions (scarce evidence) Major technical challenges for spinal cord imaging at UHF remain, eg, susceptibility effects or motion artifacts

UHF, ultra-high-field; MRI, magnetic resonance imaging; MS, multiple sclerosis; CVS, central vein sign; LME, leptomeningeal inflammation.

White Matter Pathology

Although UHF imaging is clearly superior for detecting cortical MS lesions, its relative sensitivity for white matter lesions is still debated (Table 1). A study using T2-FLAIR in 38 MS patients at both 3 and 7 T showed that MRI at 3 T was more sensitive to detect white matter lesions, whereas cortical lesion detection was improved at 7 T.[94] To enhance white matter lesion detection with T2-FLAIR at 7 T, magnetization-prepared 3D T2-FLAIR has been developed[95,96] and optimized.[97] This sequence seems to show at least similar sensitivity to white matter lesions at 3 and 7 T, as shown in a study comprising 6 MS patients and 15 CIS patients.[98]

More sensitive detection of white matter lesions could further improve sensitivity of MS diagnosis. This would allow a more accurate identification of white matter lesions, for example, in the optic radiation, in which MS lesion burden may correlate with retinal thinning.[99] Alternatively, it could facilitate detection of lesions within small anatomical compartments such as the optic nerves, which have been suggested as a fifth anatomical compartment to fulfill the dissemination in space dimension in the McDonald criteria.[42] More work is needed to establish valid approaches for sensitive white matter lesion detection at 7 T.

Central Vein Sign

The CVS has been proposed as an imaging biomarker to improve the speed and accuracy of MS diagnosis.[56] A recent meta-analysis has shown that up to 82% of MS lesions can have a CVS.[100] The same analysis also reported a pooled sensitivity and specificity values for MS as high as 95% and 92%, respectively (pooled for 1.5, 3, and 7 T).

The fact that a centrally located vein can be found within MS lesions was initially described by Charcot in 1868.[101] A century later, central veins were successfully visualized on MRI using T2*w images,[102] and subsequent work has demonstrated that this imaging marker allows differentiation of MS from other diseases presenting with white matter lesions (Fig. 3)[59–61,103] (reviewed in Sati et al[56]). The CVS can readily be detected on T2*w scans due to the paramagnetic nature of venous blood.[58] High spatial resolution imaging is critical for identifying such veins, because their lumens are on the order of 250 μm or less.[104] For this requirement, imaging at 7 T is well positioned.[105] Hence, it is not surprising that UHF imaging studies led the charge in assessing the CVS for facilitating differential diagnosis of MS.[103,106] Subsequent endeavors also focused on CVS imaging at 3 T,[59,61] where high resolution can also be achieved.[107] Yet, 7-T imaging offers superior conspicuity of veins due to enhanced contrast-to-noise

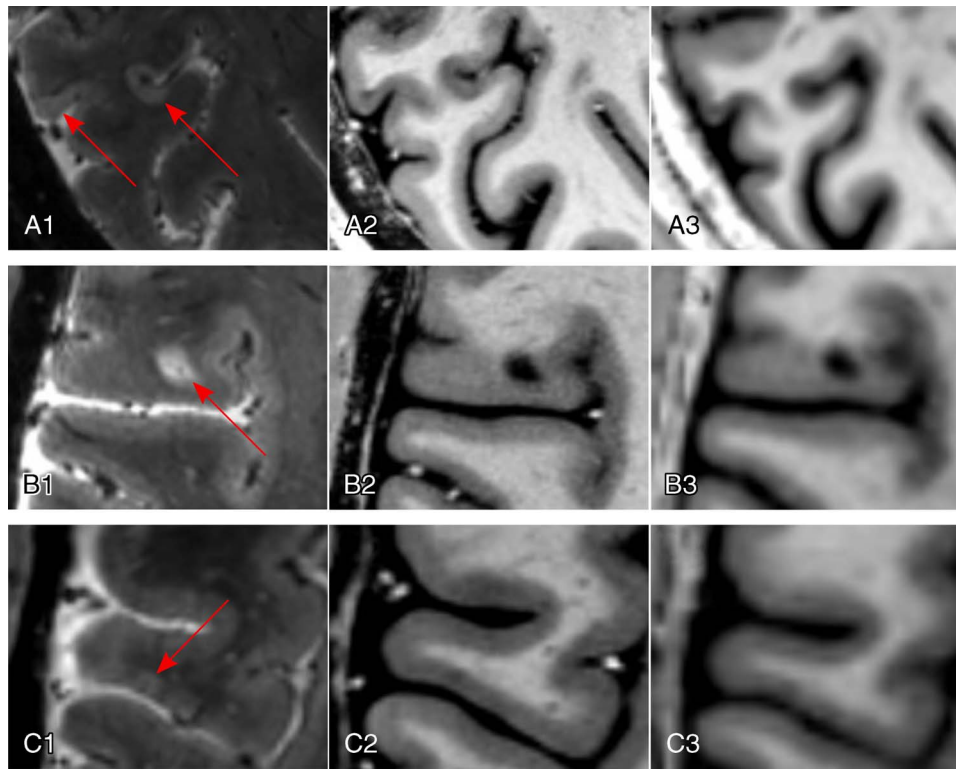

FIGURE 2. Cortical MS lesions. Ultra-high-field imaging at 7 T allows for detection of all types of cortical MS lesions (red arrows; A1–A3, subpial lesions; B1–B3, leukocortical lesion; C1–C3, intracortical lesion), exemplified using a T2*-weighted gradient echo sequence (T2*w GRE; spatial resolution, 0.5 mm isotropic) for the detection of a subpial lesion (A1), a leukocortical lesion (B1), and an intracortical lesion (C1). T1-weighted sequences, such as the magnetization prepared 2 rapid acquisition gradient echo (MP2RAGE), are also sensitive to cortical MS lesions at 7 T (A2, B2, C2; spatial resolution, 0.5 mm isotropic; average of 4 acquisitions) compared with 3 T (A3, B3, C3; spatial resolution, 1 mm isotropic; single acquisition).

ratio; this has been shown in a study comparing CVS detection in T2*w FLAIR images at 3 T (detecting 45% intralesional veins) and 7 T (detecting 87% intralesional veins).[108] This is particularly important for more difficult MS cases, for example, with only small lesions (Table 1). Based on this, several studies have taken advantage of 7 T to investigate the value of the CVS for differentiating MS from its mimics, including neuromyelitis optica spectrum disorder (NMOSD),[109] Susac syndrome,[110] and Baló's concentric sclerosis.[111] Ultra-high-field imaging has also been exploited to study the pathogenic role of veins in MS pathogenesis, that is, their link to lesion emergence.[77]

Leptomeningeal Inflammation

Leptomeningeal inflammation is not a specific MS feature, yet it offers a window into a distinct pathologic process of MS.[9] It is visualized as discrete foci of gadolinium enhancement in the leptomeningeal compartment, termed leptomeningeal enhancement (LME)[112] (Fig. 4). It is thought that LME represents local meningeal fibrosis caused by chronic or resolved inflammation and resultant trapping of a small amount of gadolinium within the subarachnoid space.[9] Alternatively, it may represent blood-meningeal barrier breakdown near sites of meningeal inflammation.[113] Interestingly, postcontrast T2-FLAIR has superior sensitivity for detecting LME compared with postcontrast T1w imaging.[114] Furthermore, a delay of at least 10 minutes after injection of contrast material is recommended to increase sensitivity for LME detection.

It is difficult to compare available studies due to considerable differences in MRI scanning protocols and patient cohorts. Therefore, it is not surprising that the reported range of LME prevalence is extremely large (1%–90%).[112,113,115–119] Patients with progressive MS seem to have higher LME prevalence, and most LME persists over years despite disease-modifying therapy.[116] Some studies showed an association between LME and cortical gray matter volume.[113] However, the association of LME with cortical pathology is still controversial.[120]

Only a handful of studies have assessed LME at 7 T in MS,[113,118,119] and none systematically compared 3- and 7-T imaging. Hence, it is currently not possible to state that 7-T imaging offers a higher sensitivity to detect LME. However, one 7-T study has identified 2 distinct patterns of LME: "nodular," that is, spherical nodules at the pial surface/subarachnoid space; and "spread/fill," that is, the appearance of contrast spreading locally through the subarachnoid space[113] (Table 1). It is noteworthy that the nodular pattern has also been observed in healthy controls,[113] although with lower prevalence than in MS. Furthermore, the true magnitude of meningeal inflammation is likely considerably higher than captured even by 7-T MRI, as shown in histopathology studies.[121] More studies are needed to elucidate the role of LME as imaging biomarker for MS.

Paramagnetic Rims and Iron Deposits

Histopathological and imaging studies have shown global alterations in iron levels in brains of MS patients.[32] Although excessive free iron can be toxic, iron also maintains integrity of myelin and oligodendrocytes, and it can be buffered inside phagocytes (macrophages and microglia). Given these conflicting effects of iron, the role of iron in MS pathophysiology remains a matter of debate.

T2*w MRI sensitively detects tissue iron, particularly at UHF imaging with its enhanced susceptibility effects. A 7-T MRI study using a 3D multiecho gradient echo (GRE) sequence to reconstruct R2* maps from brains of 2 MS patients found R2* values to be a sensitive indicator of tissue iron levels.[79] The iron sources were identified as

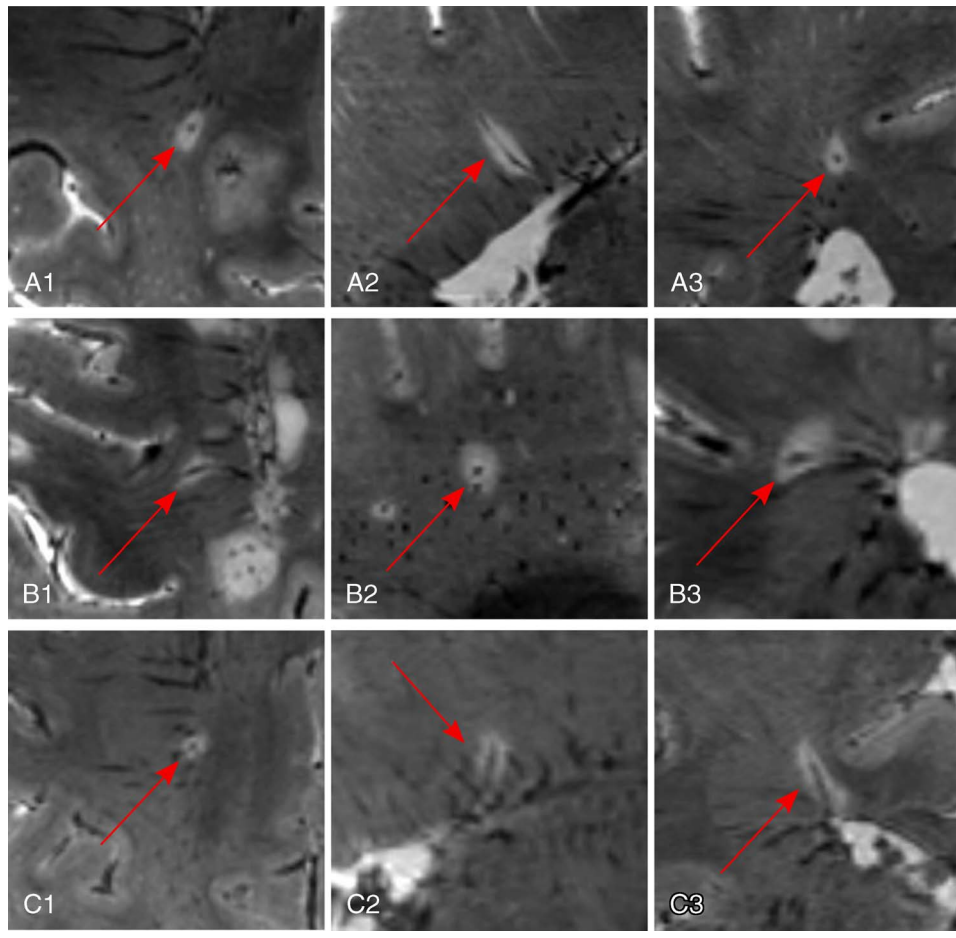

FIGURE 3. Central vein sign in MS. Ultra-high-field imaging at 7 T yields conspicuous central veins within MS lesions even when small in diameter, exemplified in 3 cases (A–C) by using a multiecho T2*w gradient echo sequence (spatial resolution, 0.5 mm isotropic). The veins are centrally located within the lesion in all 3 planes (A1, B1, C1: axial plane; A2, B2, C2: sagittal plane; A3, B3, C3: coronal plane).

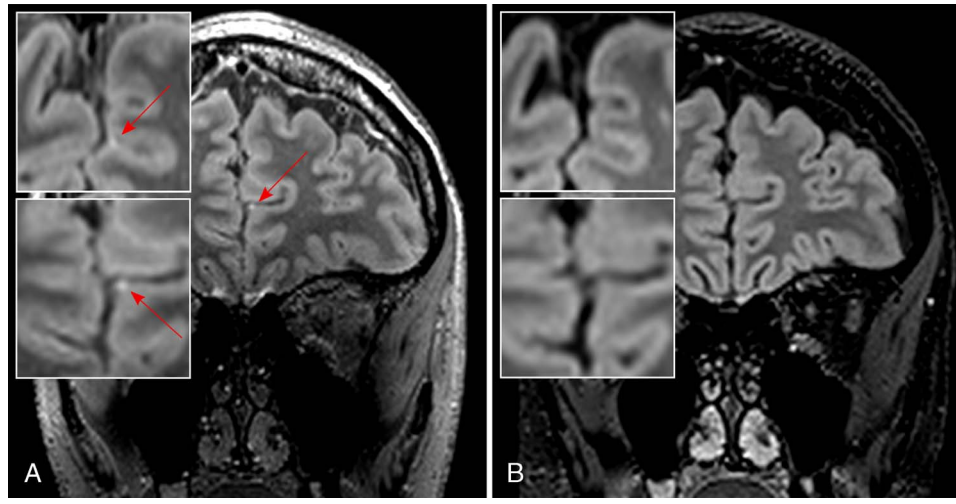

FIGURE 4. Leptomeningeal enhancement in MS. Ultra-high-field imaging at 7 T is able to sensitively detect foci of leptomeningeal enhancement (LME, red arrow) as demonstrated in this postgadolinium T2-weighted fluid-attenuated inversion recovery (T2-FLAIR; spatial resolution, 0.7 mm isotropic) sequence from a progressive MS patient with interhemispheric LME (A, with magnified axial [top] and coronal [bottom] images), which is not detected on postgadolinium T2-FLAIR images at 3 T (B, with magnified axial [top] and coronal [bottom] images). Both T2-FLAIR images were acquired ≈10 minutes after contrast medium administration.

oligodendrocytes in normal-appearing white matter and activated macrophages/microglia, particularly at the edges of white matter lesions. These iron sources were confirmed in a subsequent gene microarray study.[122]

It has been proposed that this perilesional iron, identified as paramagnetic rim (or phase rim) on MRI, is a marker of chronic active MS lesions[78,123] (Fig. 5). An UHF imaging study combining dynamic contrast-enhanced MRI with T2*w phase imaging colocalized this paramagnetic rim with the inflammatory front of new MS lesions.[78] Based on this notion, it was hypothesized that the paramagnetic rim reflects ongoing leakage of paramagnetic serum proteins. A subsequent 7-T study using dynamic contrast-enhanced MRI investigated paramagnetic rims in both centrifugally and centripetally gadolinium-enhancing lesions in 17 MS patients.[124] Only centripetally enhancing lesions showed a paramagnetic rim, and interestingly, lesions with persistent paramagnetic rims were more likely to become hypointense on T1w images within 3 to 12 months. In histopathological examination, such persistent paramagnetic rims corresponded to iron-loaded inflammatory myeloid cells at the lesion edge. Aside from their potential role in identifying active inflammation, paramagnetic rims seem to have a certain specificity to MS, as they have not been observed in vascular lesions[125] and are only rarely present in Susac syndrome.[110] However, albeit rare, they may be observed in neoplastic or infectious CNS disorders.[126,127] So far, the only study to compare the sensitivity of 3 T versus 7 T for paramagnetic rims showed similar sensitivity.[128]

Based on existing data, it seems as if local accumulation of iron within lesion edges could be used as biomarker for MS. Yet, more work is needed to elucidate the exact role of iron in MS.

Spinal Cord Imaging

Spinal cord pathology is an extremely common MS feature and is closely associated with clinical disability.[65,129] With the small dimensions of the spinal cord (diameter of 1–1.5 cm), even a minimal amount of partial volume effect is detrimental to image quality. With its ability for excellent spatial resolution and SNR, spinal cord pathology detection could benefit from UHF imaging. A comparative study at 3 and 7 T comprising 15 MS patients and 15 healthy controls showed that 7 T increases MS lesion detection by 50% by additionally offering superior details of anatomical structures such as the nerve root entry/exit zones, which can be confused for demyelination[130] (Table 1). However, technical challenges still impede efficient use of 7 T for spinal cord imaging.[131] These difficulties have different causes: first, high sensitivity to susceptibility effects at UHF induces unwarranted tissue contrast at interfaces such as the vertebral column or the lung, which are in proximity to the spinal cord. Second, physiological motion caused by the heartbeat, respiration, or bulk CSF flow leads to imaging artifacts. Third, due to the small cross-sectional area and the cylindrical shape of the spinal cord, it is difficult to establish a balance between the need for high in-plane resolution and a large field of view. Thus, while of high clinical relevance, UHF spinal cord imaging still needs substantial improvement to merit clinical implementation.

Exploring Additional Pathologic Features of Multiple Sclerosis Using Ultra-High-Field Magnetic Resonance Imaging

Other techniques have been used to further exploit increased static magnetic field strengths to explore pathogenic MS mechanisms, among them sodium (^{23}Na) imaging. Even with sodium being the most abundant cation in the human body, the MRI signal of ^{23}Na is approximately 30,000 times lower than that of protons.[132] With this, UHF imaging has been used to improve sensitivity to detect ^{23}Na in vivo. By using this technique, 1 study showed an increase in ^{23}Na in white matter of MS patients, suggesting a metabolic dysfunction of axons.[133]

Resting state functional MRI could also benefit from higher magnetic field strengths, because the bold oxygenation level-dependent signal increases supralinearly with the static magnetic field strength. However,

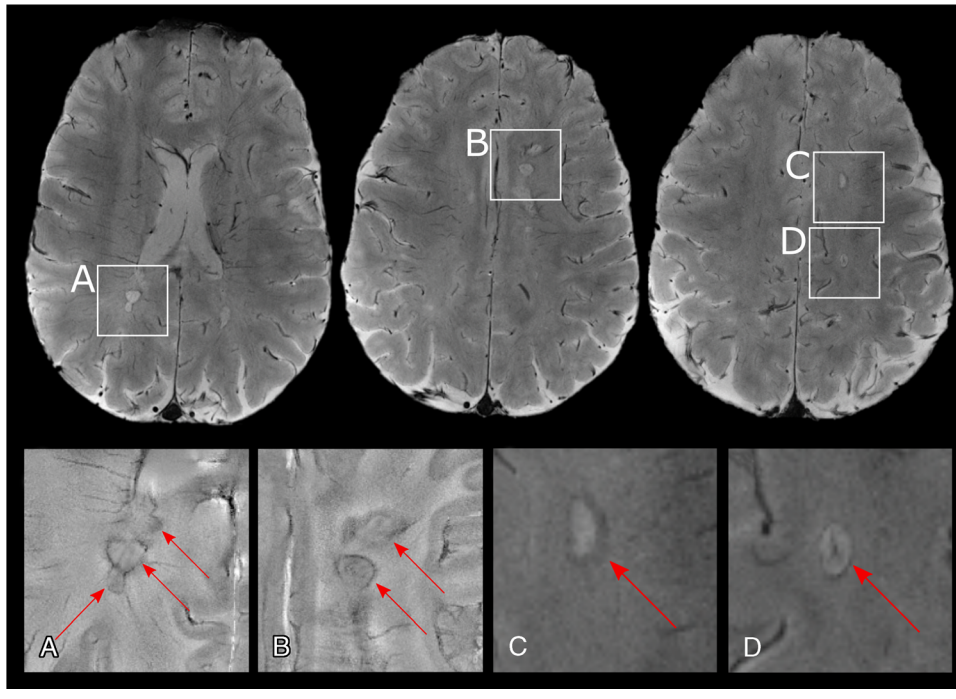

FIGURE 5. Paramagnetic rim lesions in MS. Multiple sclerosis lesions with paramagnetic rims (red arrows) are well visualized using ultra-high-field 7-T imaging, as seen in 2D gradient echo T2*-weighted magnitude (top row, C and D) and phase (insets A and B) images from an individual with progressive MS. Phase reconstructions are in general more sensitive to the paramagnetic rim than magnitude reconstructions.

heterogeneity in the radiofrequency (RF) transmission field has limited UHF fMRI for clinical use so far.[134] Furthermore, MS-related tissue changes might confound fMRI-related outcomes.

Finally, MRI spectroscopy could profit from UHF imaging via improved spectral resolution.[135] This results in an increase in the number as well as the accuracy of detected brain metabolites. By using MRI spectroscopy, 1 study found that both MS lesions and gray matter exhibit lower glutathione levels.[136] Magnetic resonance imaging spectroscopy benefits not only from improved spectral but also higher spatial resolution. This has been shown in a study applying ultra-high-resolution MRI spectroscopy ($2 \times 2 \times 8$ mm^3 voxel volume) in MS.[137] In addition, recent progress in MRI spectroscopy at 7 T, based on a free induction decay sequence, is facilitating whole-brain mapping of key metabolites in less than 3 minutes, further strengthening its potential clinical applicability.[138]

LIMITATIONS OF ULTRA-HIGH-FIELD IMAGING

Technical Challenges

Several difficulties need to be overcome for efficient clinical application of UHF MRI. Two of these challenges are particularly relevant for the clinical setting: (1) transmit and receive B1 inhomogeneities and (2) RF power deposition in tissue.[139]

First, B1 inhomogeneities are relevant for both spin echo sequences and GRE sequences, with the latter being particularly beneficial at UHF, for example, to acquire T1w images.[140] Gradient echo sequences can generate high-resolution images with high contrast and signal and low RF-energy tissue deposition. One sequence commonly used in the clinical setting is the 3D MPRAGE sequence, which can produce a 0.7-mm isometric image within approximately 6 minutes.[141] However, these T1w images are prone to B1 inhomogeneities resulting in nonuniform images.[58] One strategy to overcome B1 inhomogeneities is usage of an adiabatic inversion pulse, resulting in a more homogeneous signal.[142] Another strategy to compensate for such heterogenous signal intensities within images is acquisition of a separate proton density–weighted 3D GRE.[143] This approach has been exploited in a modification of MPRAGE, termed MP2RAGE,[144] which simultaneously acquires and combines 2 volumes at different inversion times and flip angles, resulting in a synthetic T1w image with uniform image intensity. However, the need for B1-mapping for accurate T1w image reconstruction and an acquisition time of approximately 10 minutes for 0.7 mm isotropic resolution poses a challenge for routine clinical use. Nevertheless, parallel imaging techniques have been successfully applied to shorten the acquisition time for MP2RAGE,[145,146] and therefore, shorter versions of this sequence will be available soon for clinical use.

Second, the high RF power deposition in tissue hampers the use of turbo/fast spin echo sequences for T2w images due to the multiple refocusing spin echo pulses. Therefore, to run spin echo sequences within the safety limits of specific absorption rates (SARs), slice numbers need to be decreased and/or repetition times (TRs) need to be increased. Increasing the TR to fit SAR limitations might result in very long scan times (>10 minutes) when whole-brain coverage is required. Parallel imaging and simultaneous multislice imaging can be used to achieve clinically feasible scanning times despite higher TR.[147] In addition, advances in RF transmit and receive coils will further contribute to tackling field inhomogeneities and high SAR in UHF MRI.[139] Additional optimization of both T1w and T2w sequences is warranted to realize the clinical benefits of UHF imaging.

Patient Comfort

Aside from these technical limitations, patient comfort should be considered when applying UHF MRI. Several studies have assessed subjective perception of healthy volunteers during an UHF MRI examination. The most important adverse events were dizziness, whereas moving into/out of the scanner and during scanning, which has been reported by up to one third of healthy volunteers, most likely caused by vestibular effects.[148–150] Because such symptoms depend on quick changes in the magnetic field, they can be mitigated by slower patient movement into and out of the scanner.[151] Furthermore, based on our experience scanning over 200 MS patients at 7 T, dizziness is not limiting for the majority of patients. Also, metallic taste has been reported by a minority of patients.[148]

Acoustic noise, caused by fast switching currents in the gradient coils, can also impede patient comfort.[152] Acoustic noise highly depends on engineering of gradient coils and imaging sequences used; for example, echo-planar imaging sequences can emit more than 110 dB.[153] This is further precipitated by generally tightly fitting head coils only allowing for ear plugs instead of double hearing protection. With this, one third of UHF MRI participants reported acoustic noise as importantly uncomfortable.[148] Nevertheless, overall UHF MRI seems to be well tolerated: only 3% of individuals rated such an examination as greatly unpleasant.[148]

Implanted Medical Devices

Implanted medical devices, such as pacemakers or stents, can pose a safety issue in UHF scanning. Displacement forces, torque, RF heating, and the resulting influence on image quality are all issues to consider when evaluating such devices for their compatibility with UHF.[154] To date, a few hundred metallic implants and devices have been evaluated for safety at 7 T, which is still a fraction of the more than

TABLE 2. Comparison Between Clinically Approved 7-T Scanner Systems

Manufacturer	Siemens	GE
Name	Magnetom Terra	Signa
B_0, T	7	7
Magnet weight with cryogens	Approximately 17,000 kg	Approximately 45,000 kg
Typical B_0 homogeneity 40 cm DSV	≈2 ppm peak to peak	≈3 ppm peak to peak
Helium boil of rate	Zero boil off	Zero boil off
Fringe field (axial × radial), m	7.9 × 4.95	8.0 × 4.4 at 5 gauss
Patient bore (length × width × height), cm	270 (magnet) × 60 × 60	330 × 60 × 60
Patient aperture, cm	60	60
Gradient: peak amplitude, per axis, mT/m	80	113
Gradient: peak slew-rate, per axis, T/m/s	200	260
Multinuclear imaging	Yes	Yes

GE, General Electrics.

6000 metallic items that have been tested at 3 and/or 1.5 T.[151] Although many implanted devices have still not been tested for their UHF MR eligibility, safety data are rapidly increasing and will likely facilitate its future use in the clinical setting.[151,155] Of note, it is still under debate whether implants located beyond the RF transmit coil volume pose a safety risk. According to the German Ultra-High Field Imaging Network, it is recommended that passive metallic implants distant from the transmit RF coil and labeled MR conditional for 3 T are also safe for higher static magnetic field strengths, including 7 T,[156] but clearly, more research is needed to broaden data on MRI compatibility of implanted medical devices at 7 T.

PRACTICAL ASPECTS OF 7-T IMAGING

Vendors

Currently, 2 vendors offer clinically approved 7-T MRI systems: Siemens Healthcare's Magnetom Terra, approved in October 2017 (https://www.siemens-healthineers.com/en-us/magnetic-resonance-imaging/7t-mri-scanner/magnetom-terra), and General Electric's (GE's) Signa 7.0 T, approved in November 2020 (https://www.ge.com/news/press-releases/bringing-ultra-high-field-mr-imaging-from-research-to-clinical-signa-70t-fda-cleared). Both scanner systems have comparable magnetic fringe fields and patient bores, with the GE scanner using slightly stronger magnetic field gradients (Table 2). The Siemens system is capable of multinuclear imaging, whereas the GE system also features a multinuclear spectroscopy mode.

Costs

The costs of a 7-T MRI system are considerably higher compared with 1.5- or 3-T MRI systems. The list price of a 7-T MRI system is US $7 to $10 (according to rule of thumb US $1 million per Tesla). Of note, this only covers hardware/software and the installation of the UHF machine. Additional substantial expenses come with intricate siting, taking up to several months (compared with 2–3 weeks for a 3-T device). The reduced weight of the Magnetom Terra allows installations in floors other than the ground floor. Additional costs include software, running costs, and training of personnel. It is noteworthy that a 7-T system requires more space for installation (in the range of 80–90 m^2), not least due to its relatively larger static magnetic fringe fields (axial-radial 5 gauss limits at 8×5 m). For 3-T systems, the fringe magnetic fields reach 5 gauss at approximately half the distance.[151] Mitigating the higher cost are zero helium boil-off systems, which reduce helium consumption.

NEW HORIZONS IN ULTRA-HIGH-FIELD IMAGING

In addition to the improvement of individual MRI sequences for image resolution and acquisition time, current research also aims at overcoming long scanning times and associated challenges at UHF by other means. One such endeavor is the development of software-based motion correction methods, which would tackle motion artifacts during scanning.[142] Such methods would particularly be helpful for T2*w sequences that require long echo times and are thus prone to patient motion or physiological fluctuations. One such approach used B_0 correction with a navigator-guided GRE sequence to enhance sensitivity at UHF imaging to detect cortical lesions.[157] By applying this image correction method, more than double the number of cortical lesions could be detected using a T2*w sequence. Similar techniques using navigator echoes have been applied to correct for resonance frequency variations.[158] Also, novel coil designs with built-in camera to track an optical marker have been used to overcome subject motion during scanning.[159]

Compressed sensing has been 1 of the most important breakthroughs in recent decades to reduce scanning time by accurate image reconstruction from sparsely sampled k space data.[160–162] One recent study compared a conventional SENSE-accelerated DIR with compressed SENSE DIR at 3 T in MS, thereby reducing acquisition time by over 50%.[163] Such endeavors are currently being translated to UHF imaging. This approach could preserve sensitivity to detect white matter lesions while reducing image artifacts. The recent FDA approval of compressed sensing for clinical scans further emphasizes the maturity of these techniques and their future utility for UHF imaging.[160]

Finally, also endeavors at harmonizing UHF imaging across different scanners and sites have been undertaken.[164] This could facilitate multicenter studies and improve comparability of MRI scans acquired at different clinical sites.

CONCLUSIONS

Ultra-high-field MRI offers distinct conspicuity of key pathologic MS features, among them the CVS and cortical pathology. With this, UHF imaging benefits improved specificity of MRI for MS diagnosis and potentially therapeutic monitoring. Thus, while not replacing imaging at 3 or 1.5 T within the coming years, it can complement imaging at lower field strengths, thereby likely improving confidence of MS diagnosis. Furthermore, technical progress in accelerating structural imaging and eliminating image artifacts will further broaden the purview of UHF imaging in MS patient care at academic centers. Finally, the enhanced spatial resolution and susceptibility effects of UHF imaging can further spark the discovery of new MS imaging biomarkers.

ACKNOWLEDGMENTS

The authors cordially thank Martina Absinta for providing MRIs on LME. They thank Professor Michael Weller from the University Hospital of Zurich, Department of Neurology for research support. They also thank Alan Hoofring and Steve Hillage for figure creation.

REFERENCES

1. Reich DS, Lucchinetti CF, Calabresi PA. Multiple sclerosis. *N Engl J Med*. 2018; 378:169–180.
2. Lassmann H. Multiple sclerosis pathology. *Cold Spring Harb Perspect Med*. 2018;8:a028936.
3. Trapp BD, Peterson J, Ransohoff RM, et al. Axonal transection in the lesions of multiple sclerosis. *N Engl J Med*. 1998;338:278–285.
4. Kuhlmann T, Ludwin S, Prat A, et al. An updated histological classification system for multiple sclerosis lesions. *Acta Neuropathol*. 2017;133:13–24.
5. Goldschmidt T, Antel J, König FB, et al. Remyelination capacity of the MS brain decreases with disease chronicity. *Neurology*. 2009;72:1914–1921.
6. Patrikios P, Stadelmann C, Kutzelnigg A, et al. Remyelination is extensive in a subset of multiple sclerosis patients. *Brain*. 2006;129:3165–3172.
7. Patani R, Balaratnam M, Vora A, et al. Remyelination can be extensive in multiple sclerosis despite a long disease course. *Neuropathol Appl Neurobiol*. 2007;33:277–287.
8. Taylor EW. Zur pathologischen anatomie der multiplen sklerose. *Dtsch Z Nervenheilkd*. 1894;5:1–26.
9. Zurawski J, Lassmann H, Bakshi R. Use of magnetic resonance imaging to visualize leptomeningeal inflammation in patients with multiple sclerosis: a review. *JAMA Neurol*. 2017;74:100–109.
10. Kutzelnigg A, Lucchinetti CF, Stadelmann C, et al. Cortical demyelination and diffuse white matter injury in multiple sclerosis. *Brain*. 2005;128:2705–2712.
11. Lucchinetti CF, Popescu BF, Bunyan RF, et al. Inflammatory cortical demyelination in early multiple sclerosis. *N Engl J Med*. 2011;365:2188–2197.
12. Geurts JJ, Bö L, Pouwels PJ, et al. Cortical lesions in multiple sclerosis: combined postmortem MR imaging and histopathology. *Am J Neuroradiol*. 2005; 26:572–577.
13. Pitt D, Boster A, Pei W, et al. Imaging cortical lesions in multiple sclerosis with ultra-high-field magnetic resonance imaging. *Arch Neurol*. 2010;67:812–818.
14. Kilsdonk ID, Jonkman LE, Klaver R, et al. Increased cortical grey matter lesion detection in multiple sclerosis with 7 T MRI: a post-mortem verification study. *Brain*. 2016;139:1472–1481.
15. Yao B, Hametner S, van Gelderen P, et al. 7 Tesla magnetic resonance imaging to detect cortical pathology in multiple sclerosis. *PloS One*. 2014;9:e108863.
16. Bo L, Vedeler CA, Nyland HI, et al. Subpial demyelination in the cerebral cortex of multiple sclerosis patients. *J Neuropathol Exp Neurol*. 2003;62:723–732.

17. Mainero C, Benner T, Radding A, et al. In vivo imaging of cortical pathology in multiple sclerosis using ultra-high field MRI. *Neurology*. 2009;73:941–948.
18. Calabrese M, Poretto V, Favaretto A, et al. Cortical lesion load associates with progression of disability in multiple sclerosis. *Brain*. 2012;135:2952–2961.
19. Papadopoulou A, Müller-Lenke N, Naegelin Y, et al. Contribution of cortical and white matter lesions to cognitive impairment in multiple sclerosis. *Mult Scler J*. 2013;19:1290–1296.
20. Calabrese M, Magliozzi R, Ciccarelli O, et al. Exploring the origins of grey matter damage in multiple sclerosis. *Nat Rev Neurosci*. 2015;16:147–158.
21. Kidd D, Barkhof F, McConnell R, et al. Cortical lesions in multiple sclerosis. *Brain*. 1999;122:17–26.
22. Matthews PM. Chronic inflammation in multiple sclerosis—seeing what was always there. *Nat Rev Neurol*. 2019;15:582–593.
23. Choi SR, Howell OW, Carassiti D, et al. Meningeal inflammation plays a role in the pathology of primary progressive multiple sclerosis. *Brain*. 2012;135:2925–2937.
24. Magliozzi R, Howell OW, Reeves C, et al. A gradient of neuronal loss and meningeal inflammation in multiple sclerosis. *Ann Neurol*. 2010;68:477–493.
25. Magliozzi R, Howell O, Vora A, et al. Meningeal B-cell follicles in secondary progressive multiple sclerosis associate with early onset of disease and severe cortical pathology. *Brain*. 2007;130:1089–1104.
26. Howell OW, Reeves CA, Nicholas R, et al. Meningeal inflammation is widespread and linked to cortical pathology in multiple sclerosis. *Brain*. 2011;134:2755–2771.
27. Gardner C, Magliozzi R, Durrenberger PF, et al. Cortical grey matter demyelination can be induced by elevated pro-inflammatory cytokines in the subarachnoid space of MOG-immunized rats. *Brain*. 2013;136:3596–3608.
28. Magliozzi R, Howell OW, Nicholas R, et al. Inflammatory intrathecal profiles and cortical damage in multiple sclerosis. *Ann Neurol*. 2018;83:739–755.
29. Mahad DH, Trapp BD, Lassmann H. Pathological mechanisms in progressive multiple sclerosis. *Lancet Neurol*. 2015;14:183–193.
30. Haider L, Simeonidou C, Steinberger G, et al. Multiple sclerosis deep grey matter: the relation between demyelination, neurodegeneration, inflammation and iron. *J Neurol Neurosurg Psychiatry*. 2014;85:1386–1395.
31. Yao B, Bagnato F, Matsuura E, et al. Chronic multiple sclerosis lesions: characterization with high-field-strength MR imaging. *Radiology*. 2012;262:206–215.
32. Stephenson E, Nathoo N, Mahjoub Y, et al. Iron in multiple sclerosis: roles in neurodegeneration and repair. *Nat Rev Neurol*. 2014;10:459–468.
33. Mahad DJ, Ziabreva I, Campbell G, et al. Mitochondrial changes within axons in multiple sclerosis. *Brain*. 2009;132:1161–1174.
34. Trapp BD, Stys PK. Virtual hypoxia and chronic necrosis of demyelinated axons in multiple sclerosis. *Lancet Neurol*. 2009;8:280–291.
35. Kutzelnigg A, Lassmann H. Cortical lesions and brain atrophy in MS. *J Neurol Sci*. 2005;233:55–59.
36. Amato M, Bartolozzi M, Zipoli V, et al. Neocortical volume decrease in relapsing-remitting MS patients with mild cognitive impairment. *Neurology*. 2004;63:89–93.
37. Tiberio M, Chard D, Altmann D, et al. Gray and white matter volume changes in early RRMS: a 2-year longitudinal study. *Neurology*. 2005;64:1001–1007.
38. McDonald WI, Compston A, Edan G, et al. Recommended diagnostic criteria for multiple sclerosis: guidelines from the international panel on the diagnosis of multiple sclerosis. *Ann Neurol*. 2001;50:121–127.
39. Thompson AJ, Banwell BL, Barkhof F, et al. Diagnosis of multiple sclerosis: 2017 revisions of the McDonald criteria. *Lancet Neurol*. 2018;17:162–173.
40. Brownlee WJ, Hardy TA, Fazekas F, et al. Diagnosis of multiple sclerosis: progress and challenges. *Lancet*. 2017;389:1336–1346.
41. Miller D, Barkhof F, Montalban X, et al. Clinically isolated syndromes suggestive of multiple sclerosis, part I: natural history, pathogenesis, diagnosis, and prognosis. *Lancet Neurol*. 2005;4:281–288.
42. Filippi M, Rocca MA, Ciccarelli O, et al. MRI criteria for the diagnosis of multiple sclerosis: MAGNIMS consensus guidelines. *Lancet Neurol*. 2016;15:292–303.
43. Chen J, Carletti F, Young V, et al. MRI differential diagnosis of suspected multiple sclerosis. *Clin Radiol*. 2016;71:815–827.
44. Filippi M, Preziosa P, Barkhof F, et al. Diagnosis of progressive multiple sclerosis from the imaging perspective: a review. *JAMA Neurol*. 2020.
45. Tur C, Moccia M, Barkhof F, et al. Assessing treatment outcomes in multiple sclerosis trials and in the clinical setting. *Nat Rev Neurol*. 2018;14:75–93.
46. Wattjes MP, Rovira A, Miller D, et al. Evidence-based guidelines: MAGNIMS consensus guidelines on the use of MRI in multiple sclerosis—establishing disease prognosis and monitoring patients. *Nat Rev Neurol*. 2015;11:597–606.
47. Cotton F, Weiner HL, Jolesz FA, et al. MRI contrast uptake in new lesions in relapsing-remitting MS followed at weekly intervals. *Neurology*. 2003;60:640–646.
48. Sastre-Garriga J, Pareto D, Battaglini M, et al. MAGNIMS consensus recommendations on the use of brain and spinal cord atrophy measures in clinical practice. *Nat Rev Neurol*. 2020;16:171–182.
49. Giovannoni G, Butzkueven H, Dhib-Jalbut S, et al. Brain health: time matters in multiple sclerosis. *Mult Scler Relat Disord*. 2016;9:S5–S48.
50. Solomon AJ, Corboy JR. The tension between early diagnosis and misdiagnosis of multiple sclerosis. *Nat Rev Neurol*. 2017;13:567–572.
51. Zheng Y, Shen C-H, Wang S, et al. Application of the 2017 McDonald criteria in a Chinese population with clinically isolated syndrome. *Ther Adv Neurol Disord*. 2020;13:1756286419898083.
52. Banerjee T, Saha M, Ghosh E, et al. Conversion of clinically isolated syndrome to multiple sclerosis: a prospective multi-center study in Eastern India. *Mult Scler J Exp Transl Clin*. 2019;5:2055217319849721.
53. Filippi M, Preziosa P, Banwell BL, et al. Assessment of lesions on magnetic resonance imaging in multiple sclerosis: practical guidelines. *Brain*. 2019;142:1858–1875.
54. Solomon AJ, Bourdette DN, Cross AH, et al. The contemporary spectrum of multiple sclerosis misdiagnosis: a multicenter study. *Neurology*. 2016;87:1393–1399.
55. Solomon AJ, Naismith RT, Cross AH. Misdiagnosis of multiple sclerosis: impact of the 2017 McDonald criteria on clinical practice. *Neurology*. 2019;92:26–33.
56. Sati P, Oh J, Constable RT, et al. The central vein sign and its clinical evaluation for the diagnosis of multiple sclerosis: a consensus statement from the North American imaging in multiple sclerosis cooperative. *Nat Rev Neurol*. 2016;12:714–722.
57. Absinta M, Sati P, Reich DS. Advanced MRI and staging of multiple sclerosis lesions. *Nat Rev Neurol*. 2016;12:358–368.
58. Sati P. Diagnosis of multiple sclerosis through the lens of ultra-high-field MRI. *J Magn Reson*. 2018;291:101–109.
59. Sinnecker T, Clarke MA, Meier D, et al. Evaluation of the central vein sign as a diagnostic imaging biomarker in multiple sclerosis. *JAMA Neurol*. 2019;76:1446–1456.
60. Solomon AJ, Watts R, Ontaneda D, et al. Diagnostic performance of central vein sign for multiple sclerosis with a simplified three-lesion algorithm. *Mult Scler J*. 2018;24:750–757.
61. Maggi P, Absinta M, Grammatico M, et al. Central vein sign differentiates multiple sclerosis from central nervous system inflammatory vasculopathies. *Ann Neurol*. 2018;83:283–294.
62. Bouman PM, Steenwijk MD, Pouwels PJW, et al. Histopathology-validated recommendations for cortical lesion imaging in multiple sclerosis. *Brain*. 2020;143:2988–2997.
63. Calabrese M, Agosta F, Rinaldi F, et al. Cortical lesions and atrophy associated with cognitive impairment in relapsing-remitting multiple sclerosis. *Arch Neurol*. 2009;66:1144–1150.
64. Harrison DM, Roy S, Oh J, et al. Association of cortical lesion burden on 7-T magnetic resonance imaging with cognition and disability in multiple sclerosis. *JAMA Neurol*. 2015;72:1004–1012.
65. Kearney H, Miller DH, Ciccarelli O. Spinal cord MRI in multiple sclerosis—diagnostic, prognostic and clinical value. *Nat Rev Neurol*. 2015;11:327–338.
66. Clarke GD, Rahal A, Morin RL. Magnetic resonance imaging at 3 Tesla: time to begin, again. *J Am Coll Radiol*. 2004;1:524–526.
67. Trattnig S, Springer E, Bogner W, et al. Key clinical benefits of neuroimaging at 7 T. *Neuroimage*. 2018;168:477–489.
68. Pohmann R, Speck O, Scheffler K. Signal-to-noise ratio and MR tissue parameters in human brain imaging at 3, 7, and 9.4 Tesla using current receive coil arrays. *Magn Reson Med*. 2016;75:801–809.
69. Griswold MA, Jakob PM, Heidemann RM, et al. Generalized autocalibrating partially parallel acquisitions (GRAPPA). *Magn Reson Med*. 2002;47:1202–1210.
70. Pruessmann KP, Weiger M, Scheidegger MB, et al. SENSE: sensitivity encoding for fast MRI. *Magn Reson Med*. 1999;42:952–962.
71. Wiesinger F, Van de Moortele PF, Adriany G, et al. Parallel imaging performance as a function of field strength—an experimental investigation using electrodynamic scaling. *Magn Reson Med*. 2004;52:953–964.
72. Redpath TW. Signal-to-noise ratio in MRI. *Br J Radiol*. 1998;71:704–707.
73. Laader A, Beiderwellen K, Kraff O, et al. 1.5 versus 3 versus 7 Tesla in abdominal MRI: a comparative study. *PloS One*. 2017;12:e0187528.
74. Duyn JH, van Gelderen P, Li T-Q, et al. High-field MRI of brain cortical substructure based on signal phase. *Proc Natl Acad Sci*. 2007;104:11796–11801.

75. Reichenbach JR, Venkatesan R, Schillinger DJ, et al. Small vessels in the human brain: MR venography with deoxyhemoglobin as an intrinsic contrast agent. *Radiology*. 1997;204:272–277.
76. Haacke EM, Cheng NY, House MJ, et al. Imaging iron stores in the brain using magnetic resonance imaging. *Magn Reson Imaging*. 2005;23:1–25.
77. Dal-Bianco A, Hametner S, Grabner G, et al. Veins in plaques of multiple sclerosis patients—a longitudinal magnetic resonance imaging study at 7 Tesla. *Eur Radiol*. 2015;25:2913–2920.
78. Absinta M, Sati P, Gaitan MI, et al. Seven-Tesla phase imaging of acute multiple sclerosis lesions: a new window into the inflammatory process. *Ann Neurol*. 2013;74:669–678.
79. Bagnato F, Hametner S, Yao B, et al. Tracking iron in multiple sclerosis: a combined imaging and histopathological study at 7 Tesla. *Brain*. 2011; 134:3602–3615.
80. Bruschi N, Boffa G, Inglese M. Ultra-high-field 7-T MRI in multiple sclerosis and other demyelinating diseases: from pathology to clinical practice. *Eur Radiol Exp*. 2020;4:59.
81. van Munster CE, Jonkman LE, Weinstein HC, et al. Gray matter damage in multiple sclerosis: impact on clinical symptoms. *Neuroscience*. 2015;303:446–461.
82. Nielsen AS, Kinkel RP, Tinelli E, et al. Focal cortical lesion detection in multiple sclerosis: 3 Tesla DIR versus 7 Tesla FLASH-T2. *J Magn Reson Imaging*. 2012; 35:537–542.
83. Maranzano J, Dadar M, Rudko D, et al. Comparison of multiple sclerosis cortical lesion types detected by multicontrast 3 T and 7 T MRI. *Am J Neuroradiol*. 2019; 40:1162–1169.
84. Kilsdonk ID, de Graaf WL, Soriano AL, et al. Multicontrast MR imaging at 7 T in multiple sclerosis: highest lesion detection in cortical gray matter with 3D-FLAIR. *Am J Neuroradiol*. 2013;34:791–796.
85. Tallantyre EC, Morgan PS, Dixon JE, et al. 3 Tesla and 7 Tesla MRI of multiple sclerosis cortical lesions. *J Magn Reson Imaging*. 2010;32:971–977.
86. Beck ES, Gai N, Filippini S, et al. Inversion recovery susceptibility weighted imaging with enhanced T2 weighting at 3 T improves visualization of subpial cortical multiple sclerosis lesions. *Invest Radiol*. 2020;55:727–735.
87. Beck ES, Sati P, Sethi V, et al. Improved visualization of cortical lesions in multiple sclerosis using 7 T MP2RAGE. *AJNR Am J Neuroradiol*. 2018;39: 459–466.
88. Fischer MT, Wimmer I, Höftberger R, et al. Disease-specific molecular events in cortical multiple sclerosis lesions. *Brain*. 2013;136:1799–1815.
89. Fartaria MJ, Sati P, Todea A, et al. Automated detection and segmentation of multiple sclerosis lesions using ultra-high-field MP2RAGE. *Invest Radiol*. 2019;54: 356–364.
90. Mainero C, Louapre C, Govindarajan ST, et al. A gradient in cortical pathology in multiple sclerosis by in vivo quantitative 7 T imaging. *Brain*. 2015;138: 932–945.
91. Treaba CA, Granberg TE, Sormani MP, et al. Longitudinal characterization of cortical lesion development and evolution in multiple sclerosis with 7.0-T MRI. *Radiology*. 2019;291:740–749.
92. Houtchens MK, Benedict RH, Killiany R, et al. Thalamic atrophy and cognition in multiple sclerosis. *Neurology*. 2007;69:1213–1323.
93. Kollia K, Maderwald S, Putzki N, et al. First clinical study on ultra-high-field MR imaging in patients with multiple sclerosis: comparison of 1.5 T and 7 T. *Am J Neuroradiol*. 2009;30:699–702.
94. de Graaf WL, Kilsdonk ID, Lopez-Soriano A, et al. Clinical application of multi-contrast 7-T MR imaging in multiple sclerosis: increased lesion detection compared to 3 T confined to grey matter. *Eur Radiol*. 2013;23:528–540.
95. de Graaf WL, Zwanenburg JJ, Visser F, et al. Lesion detection at seven Tesla in multiple sclerosis using magnetisation prepared 3D-FLAIR and 3D-DIR. *Eur Radiol*. 2012;22:221–231.
96. Visser F, Zwanenburg JJ, Hoogduin JM, et al. High-resolution magnetization-prepared 3D-FLAIR imaging at 7.0 Tesla. *Magn Reson Med*. 2010;64:194–202.
97. Saranathan M, Tourdias T, Kerr AB, et al. Optimization of magnetization-prepared 3-dimensional fluid attenuated inversion recovery imaging for lesion detection at 7 T. *Invest Radiol*. 2014;49:290–298.
98. Chou IJ, Lim SY, Tanasescu R, et al. Seven-Tesla magnetization transfer imaging to detect multiple sclerosis white matter lesions. *J Neuroimaging*. 2018;28: 183–290.
99. Grazioli E, Zivadinov R, Weinstock-Guttman B, et al. Retinal nerve fiber layer thickness is associated with brain MRI outcomes in multiple sclerosis. *J Neurol Sci*. 2008;268:12–17.
100. Castellaro M, Tamanti A, Pisani AI, et al. The use of the central vein sign in the diagnosis of multiple sclerosis: a systematic review and meta-analysis. *Diagnostics*. 2020;10:1025.
101. Charcot J. Leçons de 1868; Manuscrits des leçons de JM Charcot. In: *Fonds Numérisé Charcot*. Bibliothèque de l'Université Pierre & Marie Curie. 1868.
102. Tan IL, van Schijndel RA, Pouwels PJ, et al. MR venography of multiple sclerosis. *AJNR Am J Neuroradiol*. 2000;21:1039–1042.
103. Tallantyre EC, Dixon JE, Donaldson I, et al. Ultra-high-field imaging distinguishes MS lesions from asymptomatic white matter lesions. *Neurology*. 2011; 76:534–539.
104. Hooshmand I, Rosenbaum A, Stein R. Radiographic anatomy of normal cerebral deep medullary veins: criteria for distinguishing them from their abnormal counterparts. *Neuroradiology*. 1974;7:75–84.
105. Duyn JH. Studying brain microstructure with magnetic susceptibility contrast at high-field. *Neuroimage*. 2018;168:152–161.
106. Tallantyre E, Brookes M, Dixon J, et al. Demonstrating the perivascular distribution of MS lesions in vivo with 7-Tesla MRI. *Neurology*. 2008;70:2076–2078.
107. Sati P, Thomasson D, Li N, et al. Rapid, high-resolution, whole-brain, susceptibility-based MRI of multiple sclerosis. *Mult Scler J*. 2014;20: 1464–1470.
108. Tallantyre EC, Morgan PS, Dixon JE, et al. A comparison of 3 T and 7 T in the detection of small parenchymal veins within MS lesions. *Invest Radiol*. 2009;44: 491–494.
109. Sinnecker T, Dörr J, Pfueller CF, et al. Distinct lesion morphology at 7-T MRI differentiates neuromyelitis optica from multiple sclerosis. *Neurology*. 2012;79: 708–714.
110. Wuerfel J, Sinnecker T, Ringelstein EB, et al. Lesion morphology at 7 Tesla MRI differentiates Susac syndrome from multiple sclerosis. *Mult Scler J*. 2012;18: 1592–1599.
111. Behrens JR, Wanner J, Kuchling J, et al. 7 Tesla MRI of Balo's concentric sclerosis versus multiple sclerosis lesions. *Ann Clin Transl Neurol*. 2018;5:900–912.
112. Eisele P, Griebe M, Szabo K, et al. Investigation of leptomeningeal enhancement in MS: a postcontrast FLAIR MRI study. *Neurology*. 2015;84:770–775.
113. Harrison DM, Wang KY, Fiol J, et al. Leptomeningeal enhancement at 7 T in multiple sclerosis: frequency, morphology, and relationship to cortical volume. *J Neuroimaging*. 2017;27:461–468.
114. Singh SK, Agris JM, Leeds NE, et al. Intracranial leptomeningeal metastases: comparison of depiction at FLAIR and contrast-enhanced MR imaging. *Radiology*. 2000;217:50–53.
115. Zivadinov R, Ramasamy DP, Vaneckova M, et al. Leptomeningeal contrast enhancement is associated with progression of cortical atrophy in MS: a retrospective, pilot, observational longitudinal study. *Mult Scler J*. 2017;23:1336–1345.
116. Absinta M, Cortese IC, Vuolo L, et al. Leptomeningeal gadolinium enhancement across the spectrum of chronic neuroinflammatory diseases. *Neurology*. 2017;88: 1439–1444.
117. Titelbaum DS, Engisch R, Schwartz ED, et al. Leptomeningeal enhancement on 3D-FLAIR MRI in multiple sclerosis: systematic observations in clinical practice. *J Neuroimaging*. 2020;30:917–929.
118. Absinta M, Vuolo L, Rao A, et al. Gadolinium-based MRI characterization of leptomeningeal inflammation in multiple sclerosis. *Neurology*. 2015;85:18–28.
119. Ighani M, Jonas S, Izbudak I, et al. No association between cortical lesions and leptomeningeal enhancement on 7-Tesla MRI in multiple sclerosis. *Mult Scler*. 2020;26:165–176.
120. Absinta M, Ontaneda D. *Controversial Association Between Leptomeningeal Enhancement and Demyelinated Cortical Lesions in Multiple Sclerosis*. London, United Kingdom: SAGE Publications Sage UK; 2020;26:135–136.
121. Haider L, Zrzavy T, Hametner S, et al. The topograpy of demyelination and neurodegeneration in the multiple sclerosis brain. *Brain*. 2016;139:807–815.
122. Hametner S, Wimmer I, Haider L, et al. Iron and neurodegeneration in the multiple sclerosis brain. *Ann Neurol*. 2013;74:848–861.
123. Hammond KE, Metcalf M, Carvajal L, et al. Quantitative in vivo magnetic resonance imaging of multiple sclerosis at 7 Tesla with sensitivity to iron. *Ann Neurol*. 2008;64:707–713.
124. Absinta M, Sati P, Schindler M, et al. Persistent 7-Tesla phase rim predicts poor outcome in new multiple sclerosis patient lesions. *J Clin Invest*. 2016;126: 2597–2609.
125. Kilsdonk ID, Wattjes MP, Lopez-Soriano A, et al. Improved differentiation between MS and vascular brain lesions using FLAIR* at 7 Tesla. *Eur Radiol*. 2014;24:841–849.
126. Absinta M, Reich DS, Filippi M. Spring cleaning: time to rethink imaging research lines in MS? *J Neurol*. 2016;263:1893–1902.
127. Maggi P, Sati P, Nair G, et al. Paramagnetic rim lesions are specific to multiple sclerosis: an international multicenter 3 T MRI study. *Ann Neurol*. 2020;88: 1034–1042.
128. Absinta M, Sati P, Fechner A, et al. Identification of chronic active multiple sclerosis lesions on 3 T MRI. *Am J Neuroradiol*. 2018;39:1233–1238.

129. Ouellette R, Treaba CA, Granberg T, et al. 7 T imaging reveals a gradient in spinal cord lesion distribution in multiple sclerosis. *Brain*. 2020;143:2973–2987.
130. Dula AN, Pawate S, Dortch RD, et al. Magnetic resonance imaging of the cervical spinal cord in multiple sclerosis at 7 T. *Mult Scler J*. 2016;22:320–328.
131. Barry RL, Vannesjo SJ, By S, et al. Spinal cord MRI at 7 T. *Neuroimage*. 2018; 168:437–451.
132. Madelin G, Lee J-S, Regatte RR, et al. Sodium MRI: methods and applications. *Prog Nucl Magn Reson Spectrosc*. 2014;79:14–47.
133. Petracca M, Vancea RO, Fleysher L, et al. Brain intra-and extracellular sodium concentration in multiple sclerosis: a 7 T MRI study. *Brain*. 2016;139:795–806.
134. Gras V, Poser BA, Wu X, et al. Optimizing BOLD sensitivity in the 7 T human connectome project resting-state fMRI protocol using plug-and-play parallel transmission. *Neuroimage*. 2019;195:1–10.
135. Henning A. Proton and multinuclear magnetic resonance spectroscopy in the human brain at ultra-high field strength: a review. *Neuroimage*. 2018;168:181–198.
136. Srinivasan R, Ratiney H, Hammond-Rosenbluth KE, et al. MR spectroscopic imaging of glutathione in the white and gray matter at 7 T with an application to multiple sclerosis. *Magn Reson Imaging*. 2010;28:163–170.
137. Heckova E, Strasser B, Hangel GJ, et al. 7 T magnetic resonance spectroscopic imaging in multiple sclerosis: how does spatial resolution affect the detectability of metabolic changes in brain lesions? *Invest Radiol*. 2019;54:247–254.
138. Hingerl L, Strasser B, Moser P, et al. Clinical high-resolution 3D-MR spectroscopic imaging of the human brain at 7 T. *Invest Radiol*. 2020;55:239–248.
139. Kraff O, Quick HH. 7 T: physics, safety, and potential clinical applications. *J Magn Reson Imaging*. 2017;46:1573–1589.
140. Traboulsee A, Simon J, Stone L, et al. Revised recommendations of the consortium of MS centers task force for a standardized MRI protocol and clinical guidelines for the diagnosis and follow-up of multiple sclerosis. *Am J Neuroradiol*. 2016;37:394–401.
141. Mugler JP III, Brookeman JR. Three-dimensional magnetization-prepared rapid gradient-echo imaging (3D MP RAGE). *Magn Reson Med*. 1990;15:152–157.
142. Aldusary N, Michels L, Traber GL, et al. Lateral geniculate nucleus volumetry at 3 T and 7 T: four different optimized magnetic-resonance-imaging sequences evaluated against a 7 T reference acquisition. *Neuroimage*. 2019;186:399–409.
143. Van de Moortele PF, Auerbach EJ, Olman C, et al. T1 weighted brain images at 7 Tesla unbiased for proton density, T2∗ contrast and RF coil receive B1 sensitivity with simultaneous vessel visualization. *Neuroimage*. 2009;46:432–446.
144. Marques JP, Kober T, Krueger G, et al. MP2RAGE, a self bias-field corrected sequence for improved segmentation and T1-mapping at high field. *Neuroimage*. 2010;49:1271–1281.
145. Brenner D, Stirnberg R, Pracht ED, et al. Two-dimensional accelerated MP-RAGE imaging with flexible linear reordering. *MAGMA*. 2014;27:455–462.
146. Shin W, Shin T, Oh SH, et al. CNR improvement of MP2RAGE from slice encoding directional acceleration. *Magn Reson Imaging*. 2016;34:779–784.
147. Barth M, Breuer F, Koopmans PJ, et al. Simultaneous multislice (SMS) imaging techniques. *Magn Reson Med*. 2016;75:63–81.
148. Versluis MJ, Teeuwisse WM, Kan HE, et al. Subject tolerance of 7 T MRI examinations. *J Magn Reson Imaging*. 2013;38:722–725.
149. Heilmaier C, Theysohn JM, Maderwald S, et al. A large-scale study on subjective perception of discomfort during 7 and 1.5 T MRI examinations. *Bioelectromagnetics*. 2011;32:610–619.
150. Theysohn JM, Maderwald S, Kraff O, et al. Subjective acceptance of 7 Tesla MRI for human imaging. *MAGMA*. 2008;21:63.
151. Hoff MN, McKinney A 4th, Shellock FG, et al. Safety considerations of 7-T MRI in clinical practice. *Radiology*. 2019;292:509–518.
152. van Osch MJ, Webb AG. Safety of ultra-high field MRI: what are the specific risks? *Curr Radiol Rep*. 2014;2:61.
153. Schmitter S, Mueller M, Semmler W, et al. Maximum sound pressure levels at 7 Tesla—what's all this fuss about. *Proc Intl Soc Mag Reson Med*. 2009;3029.
154. Woods TO. Standards for medical devices in MRI: present and future. *J Magn Reson Imaging*. 2007;26:1186–1189.
155. Kraff O, Quick HH. Radiofrequency coils for 7 Tesla MRI. *Top Magn Reson Imaging*. 2019;28:145–158.
156. German Ultrahigh Field Imaging. Approval of subjects for measurements at ultra-high-field MRI. 2021.
157. Liu J, Beck ES, Filippini S, et al. Navigator-guided motion and B0 correction of T2*-weighted magnetic resonance imaging improves multiple sclerosis cortical lesion detection. *Invest Radiol*. 2021.
158. Versluis M, Peeters J, van Rooden S, et al. Origin and reduction of motion and f0 artifacts in high resolution T2*-weighted magnetic resonance imaging: application in Alzheimer's disease patients. *Neuroimage*. 2010;51:1082–1088.
159. DiGiacomo P, Maclaren J, Aksoy M, et al. A within-coil optical prospective motion-correction system for brain imaging at 7 T. *Magn Reson Med*. 2020; 84:1661–1671.
160. Ye JC. Compressed sensing MRI: a review from signal processing perspective. *BMC Biomed Eng*. 2019;1:1–17.
161. Pruessmann KP, Weiger M, Börnert P, et al. Advances in sensitivity encoding with arbitrary k-space trajectories. *Magn Reson Med*. 2001;46:638–651.
162. Lustig M, Donoho D, Pauly JM. Sparse MRI: The application of compressed sensing for rapid MR imaging. *Magn Reson Med*. 2007;58:1182–1195.
163. Eichinger P, Hock A, Schön S, et al. Acceleration of double inversion recovery sequences in multiple sclerosis with compressed sensing. *Invest Radiol*. 2019; 54:319–324.
164. Clarke WT, Mougin O, Driver ID, et al. Multi-site harmonization of 7 Tesla MRI neuroimaging protocols. *Neuroimage*. 2020;206:116335.